

# DP<sup>2</sup>-VAE: Differentially Private Pre-trained Variational Autoencoders

Dihong Jiang, Guojun Zhang, Mahdi Karami, Xi Chen, Yunfeng Shao, Yaoliang Yu

August 9, 2022

## Abstract

Modern machine learning systems achieve great success when trained on large datasets. However, these datasets usually contain sensitive information (e.g. medical records, face images), leading to serious privacy concerns. Differentially private generative models (DPGMs) emerge as a solution to circumvent such privacy concerns by generating privatized sensitive data. Similar to other differentially private (DP) learners, the major challenge for DPGM is also on how to achieve a subtle balance between utility and privacy. We propose DP<sup>2</sup>-VAE, a novel training mechanism for variational autoencoders (VAE) with provable DP guarantees and improved utility via *pre-training on private data*. Under the same DP constraints, DP<sup>2</sup>-VAE minimizes the perturbation noise during training, and hence improves utility. DP<sup>2</sup>-VAE is very flexible and easily amenable to many other VAE variants. Theoretically, we study the effect of pretraining on private data. Empirically, we conduct extensive experiments on image datasets to illustrate our superiority over baselines under various privacy budgets and evaluation metrics.

## 1 Introduction

The success of modern machine learning (ML) algorithms and applications highly relies on the access to large-scale datasets [1, 2, 3]. However, there are increasing concerns on privacy leakage during the use of the data, especially the sensitive data (e.g. face images, medical records) that can be exploited by a malicious party, even though the original ML applications never intentionally do so. For example, Fredrikson et al. [4] show that an attacker, who is only given a name and the white-box access to a face recognition model, can successfully recover face images of a particular person who appears in the training set (which is also known as the model inversion attack).

Prior efforts on developing privacy-preserving techniques include naive data anonymization [5],  $k$ -anonymity [6],  $l$ -diversity [7],  $t$ -closeness [8], semantic security [9], information-theoretic privacy [10], and differential privacy (DP) [11], where the last one is recognized as a rigorous quantization of privacy, and becomes the gold-standard in current ML community. Abadi et al. [12] propose DP-SGD algorithm, which then becomes the standard technique to train a DP learner. The core steps of DP-SGD are clipping gradient norm and injecting Gaussian noise to the gradient.

Differentially private generative model (DPGM) aims to generate synthetic data that are distributionally similar to the private data while satisfying differential privacy guarantee, so that no one can infer private information from the generation. The major benefits of DPGMs are two-fold: (1) As a proxy for releasing private data; (2) Benefiting private data analysis tasks (e.g. data querying, ML tasks), i.e. one can generate as much synthetic data as desired for data analysis tasks with DPGMs without incurring further privacy cost, as ensured by the post-processing theorem [13].

Generative adversarial network (GAN) [14] attracts most attention in developing DPGMs [15, 16, 17, 18, 19, 20], while the related works based on variational autoencoder (VAE) [21] are relatively limited [22, 23, 24]. Among related works, G-PATE [18] first notes that in order to learn a DP generator, it is not necessary to make the discriminator DP, because only the generator will be released. This idea is also utilized by GS-WGAN [20]. We found that VAE is a natural model to be considered for further exploring this idea, because only the decoder of VAE needs to be released. Our additional motivation for considering VAE over GAN is *two-fold*: (1) The minimax optimization of GAN leads to training instability [25], while VAE is easier to train. (2) VAE can estimate the joint density of input and latent variables, while GAN cannot.

The privacy-utility trade-off is one of the most important challenges in DP ML systems, i.e. privacy is preserved at a cost of model utility. A line of recent works show that leveraging large public datasets (where there is little privacy leakage concern) as additional knowledge to pre-train a model which is then fine-tuned on private data with DP training algorithms can significantly improve the utility of a DP learner while keeping the same level of DP guarantee [26, 27, 28].

We remark that if the pre-training is conducted on private data, then the resulting model utility will be further improved, since the distribution shift between public and private data disappears [29]. However, DP fine-tuning a non-privately pretrained model in a straightforward manner may still violate DP guarantees (see Remark 2.1). How to pre-train on private data without breaching DP guarantee thus remains a tantalizing open question. In this work, we give a positive answer to this question by proposing a novel mechanism for training a differentially private pretrained (conditional) VAE (DP<sup>2</sup>-VAE).

Another common challenge of related works is that most of them fail to scale well on small privacy budgets, i.e. they only yield acceptable generations when  $\epsilon = 10$ . We note that according to  $\epsilon$ -DP definition (given in Section 2), the privacy protection becomes weak when  $\epsilon = 10$  or above, because the ratio of two probabilities is upper bounded by  $\exp(10) \approx 2.2 \times 10^4$ , whereas they are presumed to be comparable for practical deployment, i.e. a DP model with smaller  $\epsilon$  (e.g.  $\epsilon = 1$  or below) provides stronger privacy protection. Our contributions can be summarized as follows:

- We theoretically and empirically study the effect of pretraining on private data for developing DP learners.
- By leveraging (part of) the pre-trained model on private data, we propose a novel mechanism for training a differentially private (conditional) VAE.
- With vanilla VAE architectures, our method yields state-of-the-art (SoTA) performance on model utility under the same  $(\epsilon, \delta)$ -DP constraint. Moreover, our method indicates more robustness and scalability on different datasets and different DP constraints.

## 2 Preliminary

In this section, we recall background knowledge in differential privacy.

### 2.1 Differential privacy

Differential privacy is widely regarded as a rigorous quantization of privacy, which upper bounds the deviation in the output distribution of a randomized algorithm given incremental deviation in input. Formally, we have the following definition:

**Definition 2.1** ( $(\epsilon, \delta)$ -DP [13]). A randomized mechanism  $\mathcal{M} : \mathcal{D} \rightarrow \mathcal{R}$  with domain  $\mathcal{D}$  and range  $\mathcal{R}$  satisfies  $(\epsilon, \delta)$ -differential privacy if for any two adjacent inputs  $d, d' \in \mathcal{D}$  and for any subset of outputs  $\mathcal{S} \subseteq \mathcal{R}$  it holds that

$$\Pr[\mathcal{M}(d) \in \mathcal{S}] \leq \exp(\epsilon) \cdot \Pr[\mathcal{M}(d') \in \mathcal{S}] + \delta \tag{1}$$

where adjacent inputs (a.k.a. neighbouring datasets) only differ in one entry. Particularly, when  $\delta = 0$ , we say that  $\mathcal{M}$  is  $\epsilon$ -DP.

A famous theorem, i.e. post-processing theorem, which is utilized by existing works (as well as ours) for proving DP guarantee of a published model, is given by:

**Theorem 2.1** (Post-processing theorem, [13]). If  $\mathcal{M}$  satisfies  $(\epsilon, \delta)$ -DP,  $F \circ \mathcal{M}$  will satisfy  $(\epsilon, \delta)$ -DP for any function  $F$  with  $\circ$  denoting the composition operator.

### 2.2 Rényi differential privacy (RDP)

Rényi differential privacy (RDP) extends ordinary DP using Rényi’s  $\alpha$  divergence [30] and provides tighter and easier composition property than the ordinary DP notion. Formally, we recall

**Definition 2.2** ( $(\alpha, \epsilon)$ -RDP [31]). A randomised mechanism  $\mathcal{M}$  is  $(\alpha, \epsilon)$ -RDP if for all adjacent inputs  $D, D'$ , Rényi's  $\alpha$ -divergence (of order  $\alpha > 1$ ) between the distribution of  $\mathcal{M}(D, \text{AUX})$  and  $\mathcal{M}(D', \text{AUX})$  satisfies:

$$\mathbb{D}_\alpha(\mathcal{M}(D, \text{AUX}) \parallel \mathcal{M}(D', \text{AUX})) := \frac{1}{\alpha-1} \log \mathbb{E}_{Z \sim Q} \left( \frac{P(Z)}{Q(Z)} \right)^\alpha \leq \epsilon, \quad (2)$$

where  $P$  and  $Q$  are the density of  $\mathcal{M}(D, \text{AUX})$  and  $\mathcal{M}(D', \text{AUX})$ , respectively (w.r.t. some dominating measure  $\mu$ ), and  $\text{AUX}$  denotes auxiliary input (could be omitted if not applicable).

Importantly, a mechanism satisfying  $(\alpha, \epsilon)$ -RDP also satisfies  $(\epsilon + \frac{\log 1/\delta}{\alpha-1}, \delta)$ -DP for any  $\delta \in (0, 1)$ .

Conveniently, RDP is linearly composable:

**Theorem 2.2** (Composition of RDP [31]). If mechanism  $\mathcal{M}_i$  satisfies  $(\alpha, \epsilon_i)$ -RDP for  $i = 1, 2, \dots, k$ , then releasing the composed mechanism  $(\mathcal{M}_1, \dots, \mathcal{M}_k)$  satisfies  $(\alpha, \sum_{i=1}^k \epsilon_i)$ -RDP.

We remark that  $(\alpha, \infty)$ -RDP (or  $(\infty, \delta)$ -DP) is not a rigorous notion to denote non-private mechanisms, because  $\epsilon$  only tracks the upper bound of privacy loss. We call a model  $\mathcal{M}$  non-private if for any  $\epsilon > 0$ , there exist adjacent inputs  $D, D'$  such that

$$\mathbb{D}_\alpha(\mathcal{M}(D, \text{AUX}) \parallel \mathcal{M}(D', \text{AUX})) > \epsilon. \quad (3)$$

First, composing a fine-tuning mechanism (either DP or not) with a non-private model remains non-private. Formally, we have:

**Theorem 2.3.** Let  $\mathcal{M}_p(D)$  denote a non-private (pre-trained) model,  $\mathcal{F}$  denote any (fine-tuning) mechanism (differentially private or not). Then, the composition  $\mathcal{M}_r(D) := (\mathcal{M}_p(D), \mathcal{F}(D, \mathcal{M}_p(D)))$  remains non-private.

See Appendix A for the proof. Theorem 2.3 formalizes the intuition that releasing *more* information (as in the composed mechanism  $\mathcal{M}_r$ , which releases both the output of  $\mathcal{F}$  and  $\mathcal{M}_p$ ) can only make one's mechanism *less* (differentially) private, while Theorem 2.2 shows that it degrades the privacy guarantee at most linearly.

However, what we are actually interested in is whether (DP) fine-tuning a non-private model violates DP guarantee, i.e. releasing  $\mathcal{F}(D, \mathcal{M}_p(D))$  instead of releasing output of both  $\mathcal{F}$  and  $\mathcal{M}_p$  in the composition is DP or not. Here we remark that DP fine-tuning a non-private model may still be non-private:

**Remark 2.1.** Let  $\mathcal{F}$  denote a DP mechanism, and  $\mathcal{M}_p(D)$  denote a non-private model.  $\mathcal{F}(D, \mathcal{M}_p(D))$  can still be non-private.

We can construct two examples to illustrate the remark.

- Consider a DP  $\mathcal{F}$  as  $\mathcal{F}(D, \text{AUX}) = c$ , where  $c$  is a constant. Then  $\mathcal{F}(D, \mathcal{M}_p(D)) = c$  is private.
- Consider a DP  $\mathcal{F}$  as  $\mathcal{F}(D, \text{AUX}) = \text{AUX}$ . Then  $\mathcal{F}(D, \mathcal{M}_p(D)) = \mathcal{M}_p(D)$  is non-private.

Despite the pessimistic result in Remark 2.1, our method, which also utilizes the idea of pre-training on private input, can *circumvent* privacy leakage by explicitly decomposing pre-trained model into two halves, which will be explained in the end of Section 3.

In our work, we also adopt the Gaussian mechanism for achieving RDP:

**Definition 2.3** (Gaussian mechanism for RDP [13, 31]). Let  $f : \mathcal{D} \rightarrow \mathbb{R}^p$  be an arbitrary  $p$ -dimensional function with sensitivity:

$$\Delta_2 f = \max_{D, D'} \|f(D) - f(D')\|_2 \quad (4)$$

for all adjacent datasets  $D, D' \in \mathcal{D}$ . The Gaussian mechanism  $\mathcal{M}_\sigma$  perturb the output of  $f$  with Gaussian noise:

$$\mathcal{M}_\sigma = f(D) + \mathcal{N}(0, \sigma^2 \cdot \mathbb{I}) \quad (5)$$

where  $\mathbb{I}$  is identity matrix. Then,  $\mathcal{M}_\sigma$  satisfies  $(\alpha, \frac{\alpha(\Delta_2 f)^2}{2\sigma^2})$ -RDP.

### 2.3 Variational autoencoder (VAE)

Let  $x \in \mathcal{X}$  denote data and  $z \in \mathcal{Z}$  denote latent variable. VAE consists of two components: an encoder  $T_\theta : \mathcal{X} \rightarrow \mathcal{Z}$ , where  $z = T_\theta(x) \sim q_\theta(z|x)$  ( $q_\theta(z|x)$  is known as a variational inference to approximate the intractable true posterior  $p(z|x)$ ), and a decoder  $S_\phi : \mathcal{Z} \rightarrow \mathcal{X}$ , where  $x = S_\phi(z) \sim p_\phi(x|z)$ . Given a tractable prior  $p(z)$ , e.g. Gaussian, we can rewrite  $\log p(x)$  as:

$$\log p(x) = \mathbb{E}_{q_\theta(z|x)}[\log p_\phi(x|z)] - \mathbb{D}_{KL}(q_\theta(z|x)||p(z)) + \mathbb{D}_{KL}(q_\theta(z|x)||p(z|x)) \tag{6}$$

$$\geq \mathbb{E}_{q_\theta(z|x)}[\log p_\phi(x|z)] - \mathbb{D}_{KL}(q_\theta(z|x)||p(z)) := \text{Evidence lower bound (ELBO)} \tag{7}$$

where the inequality holds due to the non-negativity of Kullback–Leibler (KL) divergence. Therefore, the training of VAE proceeds by maximizing  $\log p(x)$  via maximizing the tractable ELBO. A simple extension to conditional generation is to encode label information into the input.

## 3 Method: DP<sup>2</sup>-VAE

Our idea is inspired by GS-WGAN, where the authors warm-start (i.e. pre-train) discriminators along with a non-private generator to bootstrap the training process, and then privately train the generator while continuing normally training the pretrained discriminators, to retain differential privacy for the generator. The rationale behind it is the fact that only the generator will be released after completing the training of a GAN, so the discriminator can be non-private. We adapt this idea to VAE, where only the decoder will be released, thus it is not necessary to make the encoder private. Prior works show that subsampling can improve privacy [32, 33], so we subsample the whole training set into different subsets. Our method contains two stages. Each encoder is pretrained with a new decoder on each subset in stage 1. Proceeding to stage 2, we first reinitialize the decoder. In each training iteration, we randomly query a pre-trained encoder and its associated subsampled dataset, then privately train the decoder and normally train the encoder. Specifically, a dataset  $D$  is randomly shuffled and subsampled (without replacement) into subsets  $D_k$  (for  $k = 1, 2, \dots, K$ , we use  $K = 1000$  in this work), then the training of DP<sup>2</sup>-VAE can be summarized into two main stages:

- **Stage 1:** we reinitialize a decoder  $S_\phi$ , then pre-train both encoder  $T_{\theta_k}$  and decoder  $S_\phi$  on  $D_k$ , and save  $T_{\theta_k}$  at the end of pre-training (for  $k = 1, 2, \dots, K$ ).
- **Stage 2:** we reinitialize a decoder  $S_\phi$ . In each training iteration, we randomly query a pre-trained encoder  $T_{\theta_i}$  and associated  $D_i$ , then update parameters of  $S_\phi$  and  $T_{\theta_i}$  by private and normal training algorithms, respectively.

### 3.1 Stage 1: Pre-training encoders on private input

Stage 1 is similar to normally training a conditional VAE with gradient clipping. Differently, we partition the dataset into subsets, and each encoder is pre-trained on a subset with a reinitialized decoder. The detailed algorithm is given in Algorithm 1. The weights of pre-trained encoder in stage 1 will be transferred as input to stage 2. Note that encoders are independent of each other, so the pre-training can be conducted in parallel.

### 3.2 Stage 2: Privately training the decoder with pre-trained encoder

In stage 2, we load pre-trained encoders  $T_{\theta_k}$  ( $k = 1, 2, \dots, K$ ) obtained in stage 1. In each training iteration, we randomly query one encoder and its associated training subset, then update decoder and encoder on the subset by private and non-private training algorithms, respectively, as described in Algorithm 2.

We note that an alternative to stage 2 is to fix the pre-trained encoder. However, we empirically found that keep training the pre-trained encoder outperforms the aforementioned alternative, thus we adopt the strategy as described in this subsection in our work.

**Theorem 3.1.** Each update step in the decoder  $S_\phi$  in stage 2 satisfies  $(\alpha, \frac{2\alpha}{\sigma^2})$ -RDP.

---

**Algorithm 1:** DP<sup>2</sup>-VAE: Stage 1

---

**Input:** Private training set  $D = \{(X, y) \in \mathcal{X} \times \mathcal{Y}\}^N$ , ELBO of conditional VAE  $\mathcal{L}(X, y; \cdot, \cdot)$ , the number of pre-training iterations  $T_p$ , the number of encoders  $K$ , learning rate  $\eta_p$ , gradient clipping bound  $C$ , batch size  $B$ , Adam optimizer  $Adam(\cdot; \mathbf{aux})$

- 1 Subsample  $D$  into  $K$  subsets  $D_1, D_2, \dots, D_K$
- 2 **for**  $k \leftarrow 1$  **to**  $K$  **do**
- 3     Randomly initialize  $\theta_k, \phi$  // Initialize encoder and decoder
- 4     **for**  $t \leftarrow 1$  **to**  $T_p$  **do**
- 5         Sample a batch  $(X_b, y_b) = \{(X_i, y_i)\}_{i=1}^B \subseteq D_k$
- 6          $g_\phi(X_b, y_b) = \nabla_\phi \mathcal{L}(X_b, y_b; \theta_k, \phi)$  // Compute gradient of decoder
- 7          $g_\phi(X_b, y_b) = g_\phi(X_b, y_b) / \max(1, \frac{\|g_\phi(X_b, y_b)\|_2}{C})$  // Clip the gradient
- 8          $g_{\theta_k}(X_b, y_b) = \nabla_{\theta_k} \mathcal{L}(X_b, y_b; \theta_k, \phi)$  // Compute gradient of encoder
- 9          $g_{\theta_k}(X_b, y_b) = g_{\theta_k}(X_b, y_b) / \max(1, \frac{\|g_{\theta_k}(X_b, y_b)\|_2}{C})$  // Clip the gradient
- 10          $\phi = \phi - \eta_p * Adam(g_\phi(X_b, y_b); \mathbf{aux})$  // Update parameters of decoder
- 11          $\theta_k = \theta_k - \eta_p * Adam(g_{\theta_k}(X_b, y_b); \mathbf{aux})$  // Update parameters of encoder

**Output:**  $\theta_1, \theta_2, \dots, \theta_K$

---

We defer the proof to Appendix A.

While Remark 2.1 reveals that privacy cannot be reliably protected by trivially DP fine-tuning a non-private pre-trained model, it does not apply to DP<sup>2</sup>-VAE, even though we utilize a similar idea of pre-training on private data. The reason lies in the fact that we explicitly decompose the VAE into two halves, where only the pre-trained encoders are loaded. At the beginning of stage 2, the decoder  $S_\phi$  is randomly initialized, which eliminates private information in the pre-trained decoder, i.e.  $\phi^{(0)}$  is  $(\alpha, 0)$ -RDP. By Theorem 3.1, each decoder update step is DP, thus the released decoder  $S_\phi$  as a composition of DP mechanisms is differentially private. We provide a more intuitive interpretation to further illustrate this point: in stage 2, we first randomly initialize the decoder, then perturb the gradient with Gaussian noise when training the decoder, such that the information flow in the decoder is always privatized. The schematic of DP<sup>2</sup>-VAE is given in Appendix D.

## 4 Experiments

In this section, we evaluate and compare DP<sup>2</sup>-VAE against SoTA baselines through extensive experiments. Implementation details are given in Appendix C.

### 4.1 Experimental setup

**Datasets:** We consider three widely used image datasets, including both grayscale images (MNIST [34], Fashion MNIST [35]) and RGB images (CelebA [36]). For MNIST and Fashion MNIST, we generate images conditioned on 10 respective labels. For CelebA, we condition on gender. Description and preprocessing of the datasets are given in Appendix B.

**Evaluation tasks & metrics:** Since privacy-utility trade-off is the main concern in DP learners, we consider the following two tasks for extensive quantitative evaluations given the same set of privacy parameters (i.e. same  $(\epsilon, \delta)$ -DP) via 60k generated images:

- Generation quality, which is measured by Fréchet Inception Distance (FID) [37]. We note that FID may not be an adequate measure of generation quality, as mentioned in [38]. We still use it here as it is a standard metric when evaluating the visual fidelity of generated images.
- Model utility. We train three different classifiers, e.g. logistic regression (LR), multi-layer perceptron (MLP), and convolutional neural network (CNN), on generated images, then test the classifier on real

---

**Algorithm 2:** DP<sup>2</sup>-VAE: Stage 2

---

**Input:** Private training set  $D = \{(X, y) \in \mathcal{X} \times \mathcal{Y}\}^N$ , ELBO of conditional VAE  $\mathcal{L}(X, y; \cdot, \cdot)$ , number of training iterations  $T$ , learning rate  $\eta$ , batch size  $B$ , noise multiplier  $\sigma$ , gradient clipping bound  $C$ , the number of pre-trained encoders  $K$ , pre-trained encoder  $\theta_k$  ( $k = 1, 2, \dots, K$ ), Adam optimizer  $Adam(\cdot; \mathbf{aux})$ , DP constraint  $\delta = 10^{-5}$ , DP constraint epsilon calculator based on RDP accountant  $Eps$

```
1 Subsample  $D$  into  $K$  subsets  $D_1, D_2, \dots, D_K$  // The same as in stage 1
2 Randomly initialize  $\phi$  // Initialize decoder  $S_\phi$ 
3 for  $k \leftarrow 1$  to  $K$  do
4   Load pretrained encoder  $\theta_k$ 
5 for  $t \leftarrow 1$  to  $T$  do
6   Randomly query an index  $k \sim \text{Unif}(1, K)$ 
7   Sample a random batch  $\{(X_i, y_i)\}_{i=1}^B$  from  $D_k$ 
8   for  $i \leftarrow 1$  to  $B$  do
9      $g_\phi(X_i, y_i) = \nabla_\phi \mathcal{L}(X_i, y_i; \theta_k, \phi)$  // Compute gradient of decoder
10     $g_\phi(X_i, y_i) = g_\phi(X_i, y_i) / \max(1, \frac{\|g_\phi(X_i, y_i)\|_2}{C})$  // Clip the gradient
11     $g_{\theta_k}(X_i, y_i) = \nabla_{\theta_k} \mathcal{L}(X_i, y_i; \theta_k, \phi)$  // Compute gradient of encoder
12     $g_{\theta_k}(X_i, y_i) = g_{\theta_k}(X_i, y_i) / \max(1, \frac{\|g_{\theta_k}(X_i, y_i)\|_2}{C})$  // Clip the gradient
13     $\theta_k = \theta_k - \eta * Adam(g_{\theta_k}(X_i, y_i); \mathbf{aux})$  // Update parameters of encoder
14     $\tilde{g}_\phi = \frac{1}{B} (\sum_{i=1}^B g_\phi(X_i, y_i) + \mathcal{N}(0, \sigma^2 C^2 \mathbb{I}))$  // Gaussian mechanism
15     $\phi = \phi - \eta * Adam(\tilde{g}_\phi; \mathbf{aux})$  // Update parameters of decoder
16  $\epsilon = Eps(K, \sigma, T, \delta)$  // Calculate DP constraint  $\epsilon$ 
```

**Output:**  $\phi, \epsilon$

---

images, where the performance is measured by classification accuracy. We take 5 runs and report the average.

**SoTA baselines:** Our method is compared with following baseline methods that are also developed on image datasets, i.e. DP-CGAN [16], DP-MERF [39], Datalens [40], PATE-GAN [17], G-PATE [18], GS-WGAN [20], DP-Sinkhorn [41]. For more details, we refer interesting readers to Section 5 and respective references.

## 4.2 Comparison with SoTA baselines

We compare the proposed method with SoTA baselines through extensive qualitative and quantitative experiments on both grayscale and RGB image datasets.

### 4.2.1 Grayscale image datasets: MNIST and Fashion MNIST

As widely adopted in related works, we evaluate and compare our method with other baselines under both weak (e.g.  $\epsilon = 10$ ) and strong (e.g.  $\epsilon = 1$ ) privacy guarantees. The qualitative visualization comparison is shown in Figure 1 and Figure 2, and quantitative comparison is given in Table 1 and Table 2. To our best knowledge, among all SoTA baselines, GS-WGAN and DP-Sinkhorn generate better samples when  $\epsilon = 10$  (i.e. under  $(10, 10^{-5})$ -DP), and DataLens generates better samples when  $\epsilon = 1$  or below. While our methods also generate informative images that are comparable to some SoTA methods (e.g. GS-WGAN, DP-Sinkhorn) when  $\epsilon = 10$ , our visual improvement is more pronounced when  $\epsilon = 1$ , as shown in Figure 2.

Quantitatively, when  $\epsilon = 10$ , Table 1 indicates that our method outperforms other baselines by a significant margin in classification accuracy, and yields FID that is comparable to SoTA methods (e.g. DP-Sinkhorn). From Table 2, when  $\epsilon = 1$ , our method outperforms other baselines on both FID and CNN classification accuracy on MNIST, and achieves competitive classification accuracy on Fashion MNIST. We note that compared to  $\epsilon = 10$ , DP-MERF is the only method that achieves similar and even better evaluation



Figure 1: Qualitative comparison on MNIST and Fashion MNIST under  $(10, 10^{-5})$ -DP. Images of DP-CGAN, GS-WGAN, DP-Sinkhorn are cited from [41]. Images of G-PATE and DataLens are cited from their papers, respectively.

performance when  $\epsilon = 1$ . The authors report a similar result in their Table 9 in supplementary material, where DP-MERF under  $(1, 10^{-5})$ -DP can sometimes outperforms its non-private variant on classification tasks. However, the reason for this counter-intuitive result remains unknown.

#### 4.2.2 RGB image dataset: CelebA

To further validate the generality of our method, we also evaluate on a more complex image dataset, i.e. CelebA. Similarly, we report results under weak and strong privacy guarantees, respectively. Figure 3 shows the qualitative comparison under  $(1, 10^{-5})$ -DP, where our method generates more informative and more diverse face images than other baselines. We have similar conclusions when  $\epsilon = 10$ , which is deferred to Appendix E.1.

Additionally, Table 2 shows the quantitative comparison under  $(1, 10^{-5})$ -DP, where our method achieves comparable performance on FID and better classification accuracy compared to other SoTA baselines. Interestingly, DP-MERF achieves the best FID but the second-worst classification accuracy, which again indicates that FID may not be an ideal metric.

#### 4.3 Ablation: Pre-training on private data

To our best knowledge, GS-WGAN is the only related work that considers pretraining the model on private data. However, the authors fail to include one important ablation study, i.e. the effect of the pre-training. We conduct this experiment for GS-WGAN, and surprisingly found that the generator with the same set of default training parameters will produce nothing without pre-training the discriminators, as shown in Figure 4.

We also did this ablation for our method, as shown in Figure 5. We found that our method without pretraining encoders can generate fairly well images, which can be ascribed to the training advantage of VAE over GAN. Nevertheless, conducting pretraining still boosts the performance of the resulting decoder.

## 5 Related work

We group related work by different categories of generative models:

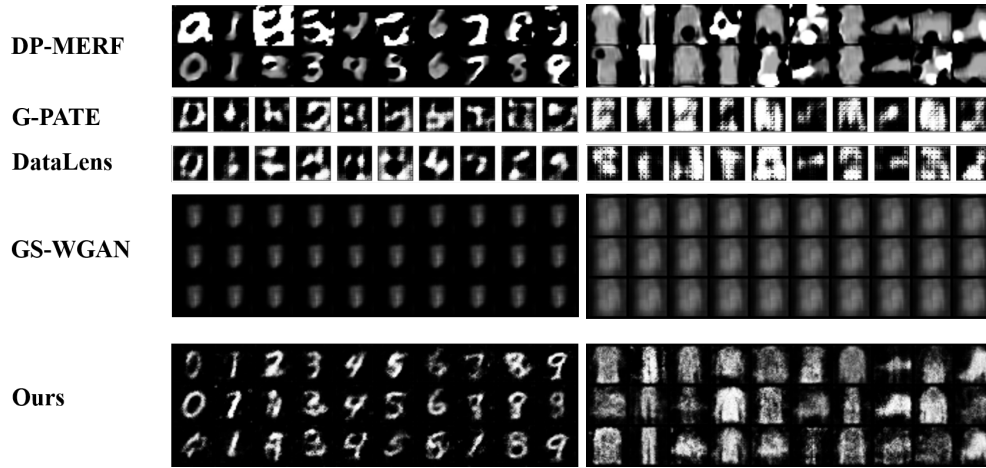


Figure 2: Qualitative comparison on MNIST and Fashion MNIST under  $(1, 10^{-5})$ -DP. Images of G-PATE and DataLens are cited from their papers, respectively.

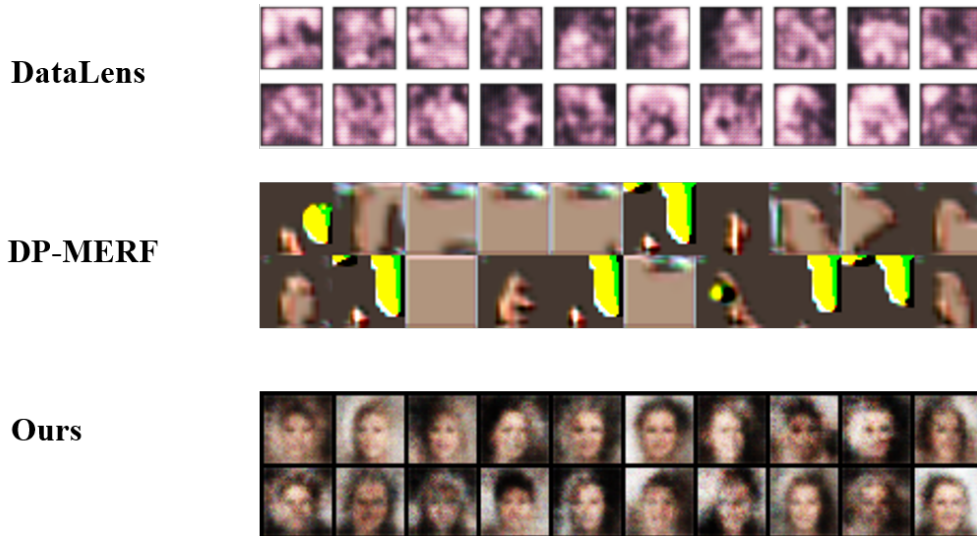


Figure 3: Qualitative comparison on CelebA conditioned on gender under  $(1, 10^{-5})$ -DP. Images of DataLens are cited from original paper. Top row: female. Bottom row: male.

Table 1: Quantitative comparison on MNIST and Fashion MNIST given  $(10, 10^{-5})$ -DP. Acc denotes classification accuracy, which is shown in %.  $\uparrow$  and  $\downarrow$  refer to higher is better or lower is better, respectively. We use boldface for the best performance. Results of DP-CGAN, GS-WGAN, DP-Sinkhorn are cited from [41]. Results of G-PATE and DataLens are cited from their papers, respectively.

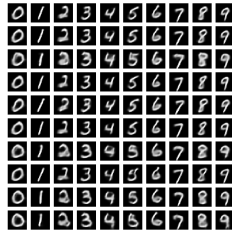
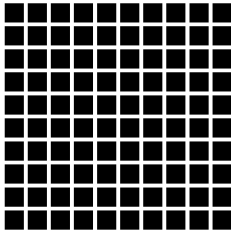
Method	$\epsilon$	MNIST				Fashion MNIST			
		FID $\downarrow$	LR Acc $\uparrow$	MLP Acc $\uparrow$	CNN Acc $\uparrow$	FID $\downarrow$	LR Acc $\uparrow$	MLP Acc $\uparrow$	CNN Acc $\uparrow$
Real data	$\infty$	1.6	92.2	97.5	99.3	2.5	84.5	88.2	90.8
DP-CGAN	10	179.2	60	60	63	243.8	51	50	46
DP-MERF	10	121.4	79.1	81.1	82.0	<b>110.4</b>	72.3	70.8	73.2
G-PATE	10	150.6	N/A	N/A	80.9	171.9	N/A	N/A	69.3
DataLens	10	173.5	N/A	N/A	80.7	167.7	N/A	N/A	70.6
GS-WGAN	10	61.3	79	79	80	131.3	68	65	65
DP-Sinkhorn ( $m = 1$ )	10	61.2	79.5	80.2	83.2	145.1	73.0	72.8	70.9
DP-Sinkhorn ( $m = 3$ )	10	<b>55.6</b>	79.1	79.2	79.1	129.4	70.2	70.2	68.9
Ours	10	67.6	<b>85.1</b>	<b>87.0</b>	<b>90.2</b>	161.6	<b>77.8</b>	<b>76.0</b>	<b>76.1</b>

Table 2: Quantitative comparison on image datasets given  $(1, 10^{-5})$ -DP. FMNIST denotes Fashion MNIST. Acc denote classification accuracy, which is shown in %.  $\uparrow$  and  $\downarrow$  refer to higher is better or lower is better, respectively. We use boldface for the best performance. Results of PATE-GAN, GS-WGAN, G-PATE are cited from [18]. Results of DataLens are cited from [40].

Dataset	Metrics	PATE-GAN	DP-MERF	GS-WGAN	G-PATE	DataLens	Ours
MNIST	FID $\downarrow$	231.5	118.3	489.8	153.4	186.1	<b>115.9</b>
	CNN Acc $\uparrow$	41.7	80.5	14.3	58.8	71.2	<b>83.2</b>
FMNIST	FID $\downarrow$	253.2	<b>102.1</b>	587.3	214.8	195.0	207.8
	CNN Acc $\uparrow$	42.22	<b>74.6</b>	16.61	58.12	64.8	71.3
CelebA	FID $\downarrow$	434.5	<b>209.6</b>	437.3	293.2	297.7	315.8
	CNN Acc $\uparrow$	44.48	58.0	62.9	70.2	70.6	<b>77.2</b>

**GAN:** The vast majority of related works are based on GAN. DP-GAN [15] first trains GAN with DP-SGD algorithm, where the discriminator is trained with DP-SGD, then the generator is automatically DP as ensured by post-processing theorem. DP-CGAN [16] extends DP-GAN into conditional generative setting. Private Aggregation of Teacher Ensembles (PATE) [42, 43] is a different mechanism for learning a DP model, and a few related works tried to apply PATE to GAN. PATE-GAN [17] trains  $k$  teacher discriminators on  $k$  disjoint partitioned datasets, and the label is predicted by aggregating teacher votes that are perturbed with Laplace noise, so that the discriminator is DP. The PATE mechanism makes the discriminator non-differentiable, thus a student discriminator is trained with teacher ensembles, which can be used to train the generator. G-PATE [18] is another work extending GAN with PATE. The authors first observed that instead of learning a DP discriminator, it suffices to ensure the information flow from the discriminator to the generator is private to make the generator DP, i.e. sanitizing the aggregated gradients from teacher discriminators to the generator. However, gradient vectors need to be discretized in each dimension to employ the PATE mechanism that only takes categorical data as input. DataLens [40] further improves G-PATE by introducing a three-step gradient compression and aggregation algorithm called TopAgg. GS-WGAN [20] explores the gradient sanitization idea from G-PATE, and applies it to training Wasserstein GAN (WGAN) with DP-SGD algorithm, so that no discretization is required.

**VAE:** DP-VaeGM [22] trains  $k$  VAEs on  $k$  classes of private data with DP-SGD algorithm, and return the union as generation. This work only evaluates their model against various privacy attacks. DP-kVAE [23] first partitions the dataset into  $k$  clusters by differentially private kernel  $k$ -means method, then trains  $k$



(a) w/o pre-training the discriminators (b) w/ pre-training the discriminators

Figure 4: The effect of pre-training discriminators in GS-WGAN on private data under  $(10, 10^{-5})$ -DP.



(a) w/o pre-training. FID = 71.1, CNN Acc = 88.3 (b) w/ pre-training. FID = 67.6, CNN Acc = 90.1

Figure 5: The effect of pre-training our method on private data under  $(10, 10^{-5})$ -DP.

VAEs on each data cluster with DP-SGD. PrivVAE designs a term-wise DP-SGD that restricts the gradient sensitivity at  $O(1)$ , because the authors observe that when additional divergence is added to the training objective of VAE as a regularization term, the gradient sensitivity will increase from  $O(1)$  to  $O(B)$  (where  $B$  is the batch size), which is not applicable to our work since we use vanilla (conditional) VAE. It is worth mentioning that both DP-VaeGM and DP-kVAE essentially directly training VAE with DP-SGD algorithm, so we think there is potential to improve DP-VAEs.

**Others:** DP-NF [44] directly trains a flow-based model by DP-SGD algorithm. DP-MERF [39] proposes to perturb embeddings (random Fourier features) of input with Gaussian noise, then training a generator by minimizing the maximum mean discrepancy (MMD) between the noisy embedding of private input and embedding of generation. DP-Sinkhorn [41] proposes to train a DP generator by minimizing the optimal transport distance between real and generated distribution with DP-SGD algorithm. There are also some DPGMs developed from graphical models, such as PrivBayes [45] and PrivSyn [46], where the idea is to use a selected set of low-degree marginals to represent a dataset (mainly low dimensional dataset such as tabular datasets), then synthesizing data from noise-perturbed marginals. However, it cannot scale well on high dimensional image datasets because the number of marginals will exponentially increase to sufficiently represent an image dataset.

## 6 Conclusion

In this paper, we propose DP<sup>2</sup>-VAE, a novel mechanism for training a differentially private (conditional) VAE on high-dimensional data. By exploring the insight that only the decoder of a VAE will be published, both pretraining encoders in stage 1 and training encoders in stage 2 can be non-private, while we only need to privately train the decoder, such that the noise perturbation in the private training is minimized, which contributes to improving the model utility under the same DP constraints. DP<sup>2</sup>-VAE can be readily extended to other variants of VAE, which is expected to benefit practical deployment. By comparing DP<sup>2</sup>-VAE with a wide range of SoTA baselines, we demonstrate the effectiveness and scalability of DP<sup>2</sup>-VAE through different datasets (both grayscale and RGB images), different privacy budgets (both strong and weak privacy constraints), and different evaluation metrics (e.g. FID and classification accuracy).

## References

- [1] Jia Deng, Wei Dong, Richard Socher, Li-Jia Li, Kai Li, and Li Fei-Fei. “**Imagenet: A large-scale hierarchical image database**”. In: *IEEE conference on computer vision and pattern recognition*. 2009, pp. 248–255.
- [2] David D Lewis, Yiming Yang, Tony Russell-Rose, and Fan Li. “**Rcv1: A new benchmark collection for text categorization research**”. *Journal of machine learning research*, vol. 5 (2004), pp. 361–397.
- [3] James Bennett, Stan Lanning, et al. “**The Netflix prize**”. In: *Proceedings of KDD cup and workshop*. 2007, p. 35.
- [4] Matt Fredrikson, Somesh Jha, and Thomas Ristenpart. “**Model inversion attacks that exploit confidence information and basic countermeasures**”. In: *Proceedings of the 22nd ACM SIGSAC conference on computer and communications security*. 2015, pp. 1322–1333.
- [5] Arvind Narayanan and Vitaly Shmatikov. “**Robust de-anonymization of large sparse datasets**”. In: *IEEE Symposium on Security and Privacy*. 2008, pp. 111–125.
- [6] Latanya Sweeney. “**k-anonymity: A model for protecting privacy**”. *International Journal of Uncertainty, Fuzziness and Knowledge-Based Systems*, vol. 10, no. 05 (2002), pp. 557–570.
- [7] Ashwin Machanavajjhala, Daniel Kifer, Johannes Gehrke, and Muthuramakrishnan Venkitasubramanian. “**l-diversity: Privacy beyond k-anonymity**”. *ACM Transactions on Knowledge Discovery from Data (TKDD)*, vol. 1, no. 1 (2007), 3–es.
- [8] Ninghui Li, Tiancheng Li, and Suresh Venkatasubramanian. “**t-closeness: Privacy beyond k-anonymity and l-diversity**”. In: *IEEE 23rd International Conference on Data Engineering*. 2007, pp. 106–115.
- [9] Shafi Goldwasser and Silvio Micali. “**Probabilistic encryption**”. *Journal of computer and system sciences*, vol. 28, no. 2 (1984), pp. 270–299.
- [10] Mario Diaz, Hao Wang, Flavio P Calmon, and Lalitha Sankar. “**On the robustness of information-theoretic privacy measures and mechanisms**”. *IEEE Transactions on Information Theory*, vol. 66, no. 4 (2019), pp. 1949–1978.
- [11] Cynthia Dwork. “**Differential privacy**”. In: *International Colloquium on Automata, Languages, and Programming*. 2006, pp. 1–12.
- [12] Martin Abadi, Andy Chu, Ian Goodfellow, H. Brendan McMahan, Ilya Mironov, Kunal Talwar, and Li Zhang. “**Deep Learning with Differential Privacy**”. In: *Proceedings of the 2016 ACM SIGSAC Conference on Computer and Communications Security*. 2016, pp. 308–318.
- [13] Cynthia Dwork, Aaron Roth, et al. “**The algorithmic foundations of differential privacy.**” *Found. Trends Theor. Comput. Sci.*, vol. 9, no. 3-4 (2014), pp. 211–407.
- [14] Ian Goodfellow, Jean Pouget-Abadie, Mehdi Mirza, Bing Xu, David Warde-Farley, Sherjil Ozair, Aaron Courville, and Yoshua Bengio. “**Generative adversarial nets**”. In: *Advances in neural information processing systems*. Vol. 27. 2014.
- [15] Liyang Xie, Kaixiang Lin, Shu Wang, Fei Wang, and Jiayu Zhou. “**Differentially Private Generative Adversarial Network**”. 2018.
- [16] Reihaneh Torkzadehmahani, Peter Kairouz, and Benedict Paten. “**DP-CGAN: Differentially Private Synthetic Data and Label Generation**”. In: *IEEE/CVF Conference on Computer Vision and Pattern Recognition Workshops (CVPRW)*. 2019, pp. 98–104.
- [17] James Jordon, Jinsung Yoon, and Mihaela Van Der Schaar. “**PATE-GAN: Generating synthetic data with differential privacy guarantees**”. In: *International conference on learning representations*. 2019.
- [18] Yunhui Long, Boxin Wang, Zhuolin Yang, Bhavya Kailkhura, Aston Zhang, Carl A. Gunter, and Bo Li. “**G-PATE: Scalable Differentially Private Data Generator via Private Aggregation of Teacher Discriminators**”. In: *Advances in Neural Information Processing Systems*. 2021.
- [19] Sean Augenstein, H. Brendan McMahan, Daniel Ramage, Swaroop Ramaswamy, Peter Kairouz, Mingqing Chen, Rajiv Mathews, and Blaise Aguerre y Arcas. “**Generative Models for Effective ML on Private, Decentralized Datasets**”. In: *International Conference on Learning Representations*. 2020.

- [20] Dingfan Chen, Tribhuvanesh Orekondy, and Mario Fritz. “GS-WGAN: A Gradient-Sanitized Approach for Learning Differentially Private Generators”. In: *Advances in Neural Information Processing Systems*. 2020, pp. 12673–12684.
- [21] Diederik P Kingma and Max Welling. “Auto-encoding variational Bayes” (2013). arXiv:1312.6114.
- [22] Qingrong Chen, Chong Xiang, Minhui Xue, Bo Li, Nikita Borisov, Dali Kaarfar, and Haojin Zhu. “Differentially Private Data Generative Models”. 2018.
- [23] Gergely Acs, Luca Melis, Claude Castelluccia, and Emiliano De Cristofaro. “Differentially private mixture of generative neural networks”. *IEEE Transactions on Knowledge and Data Engineering*, vol. 31, no. 6 (2018), pp. 1109–1121.
- [24] Tsubasa Takahashi, Shun Takagi, Hajime Ono, and Tatsuya Komatsu. “Differentially Private Variational Autoencoders with Term-wise Gradient Aggregation”. arXiv:2006.11204. 2020.
- [25] Lars Mescheder, Andreas Geiger, and Sebastian Nowozin. “Which training methods for GANs do actually converge?”. In: *International conference on machine learning*. 2018, pp. 3481–3490.
- [26] Zelun Luo, Daniel J Wu, Ehsan Adeli, and Li Fei-Fei. “Scalable differential privacy with sparse network finetuning”. In: *Proceedings of the IEEE/CVF Conference on Computer Vision and Pattern Recognition*. 2021, pp. 5059–5068.
- [27] Da Yu et al. “Differentially Private Fine-tuning of Language Models”. In: *International Conference on Learning Representations*. 2022.
- [28] Xuechen Li, Florian Tramer, Percy Liang, and Tatsunori Hashimoto. “Large Language Models Can Be Strong Differentially Private Learners”. In: *International Conference on Learning Representations*. 2022.
- [29] Olivia Wiles, Sven Gowal, Florian Stimberg, Sylvestre-Alvise Rebuffi, Ira Ktena, Krishnamurthy Dj Dvijotham, and Ali Taylan Cemgil. “A Fine-Grained Analysis on Distribution Shift”. In: *International Conference on Learning Representations*. 2022.
- [30] Alfréd Rényi. “On measures of entropy and information”. In: *Proceedings of the Fourth Berkeley Symposium on Mathematical Statistics and Probability*. Vol. 1. 1961, pp. 547–562.
- [31] Ilya Mironov. “Rényi differential privacy”. In: *IEEE 30th Computer Security Foundations Symposium (CSF)*. 2017, pp. 263–275.
- [32] Yu-Xiang Wang, Borja Balle, and Shiva Prasad Kasiviswanathan. “Subsampled rényi differential privacy and analytical moments accountant”. In: *The 22nd International Conference on Artificial Intelligence and Statistics*. 2019, pp. 1226–1235.
- [33] Borja Balle, Gilles Barthe, and Marco Gaboardi. “Privacy amplification by subsampling: Tight analyses via couplings and divergences”. In: *Advances in Neural Information Processing Systems*. Vol. 31. 2018.
- [34] Yann LeCun, Léon Bottou, Yoshua Bengio, and Patrick Haffner. “Gradient-based learning applied to document recognition”. *Proceedings of the IEEE*, vol. 86, no. 11 (1998), pp. 2278–2324.
- [35] Han Xiao, Kashif Rasul, and Roland Vollgraf. “Fashion-MNIST: a novel image dataset for benchmarking machine learning algorithms” (2017). arXiv:1708.07747.
- [36] Ziwei Liu, Ping Luo, Xiaogang Wang, and Xiaoou Tang. “Deep Learning Face Attributes in the Wild”. In: *Proceedings of International Conference on Computer Vision (ICCV)*. 2015.
- [37] Martin Heusel, Hubert Ramsauer, Thomas Unterthiner, Bernhard Nessler, and Sepp Hochreiter. “GANs trained by a two time-scale update rule converge to a local Nash equilibrium”. In: *Advances in Neural Information Processing Systems*. Vol. 30. 2017.
- [38] Mehdi SM Sajjadi, Olivier Bachem, Mario Lucic, Olivier Bousquet, and Sylvain Gelly. “Assessing generative models via precision and recall”. In: *Advances in Neural Information Processing Systems*. Vol. 31. 2018.
- [39] Frederik Harder, Kamil Adamczewski, and Mijung Park. “DP-MERF: Differentially Private Mean Embeddings with Random Features for Practical Privacy-preserving Data Generation”. In: *International Conference on Artificial Intelligence and Statistics*. 2021, pp. 1819–1827.

- [40] Boxin Wang, Fan Wu, Yunhui Long, Luka Rimanic, Ce Zhang, and Bo Li. “**DataLens: Scalable privacy preserving training via gradient compression and aggregation**”. In: *Proceedings of the ACM SIGSAC Conference on Computer and Communications Security*. 2021, pp. 2146–2168.
- [41] Tianshi Cao, Alex Bie, Arash Vahdat, Sanja Fidler, and Karsten Kreis. “**Don’t Generate Me: Training Differentially Private Generative Models with Sinkhorn Divergence**”. In: *Advances in Neural Information Processing Systems 21*. 2021.
- [42] Nicolas Papernot, Martin Abadi, Ulfar Erlingsson, Ian Goodfellow, and Kunal Talwar. “**Semi-supervised Knowledge Transfer for Deep Learning from Private Training Data**”. In: *International conference on learning representations*. 2017.
- [43] Nicolas Papernot, Shuang Song, Ilya Mironov, Ananth Raghunathan, Kunal Talwar, and Ulfar Erlingsson. “**Scalable Private Learning with PATE**”. In: *International Conference on Learning Representations*. 2018.
- [44] Chris Waites and Rachel Cummings. “**Differentially Private Normalizing Flows for Privacy-Preserving Density Estimation**”. In: *Proceedings of the AAAI/ACM Conference on AI, Ethics, and Society*. 2021, pp. 1000–1009.
- [45] Jun Zhang, Graham Cormode, Cecilia M Procopiuc, Divesh Srivastava, and Xiaokui Xiao. “**PrivBayes: Private data release via bayesian networks**”. *ACM Transactions on Database Systems (TODS)*, vol. 42, no. 4 (2017), pp. 1–41.
- [46] Zhikun Zhang, Tianhao Wang, Ninghui Li, Jean Honorio, Michael Backes, Shibo He, Jiming Chen, and Yang Zhang. “**PrivSyn: Differentially Private Data Synthesis**”. In: *30th USENIX Security Symposium (USENIX Security 21)*. 2021, pp. 929–946.
- [47] Christian Szegedy, Vincent Vanhoucke, Sergey Ioffe, Jon Shlens, and Zbigniew Wojna. “**Rethinking the inception architecture for computer vision**”. In: *Proceedings of the IEEE conference on computer vision and pattern recognition*. 2016, pp. 2818–2826.

## A Proof

**Theorem 2.3.** Let  $\mathcal{M}_p(D)$  denote a non-private (pre-trained) model,  $\mathcal{F}$  denote any (fine-tuning) mechanism (differentially private or not). Then, the composition  $\mathcal{M}_r(D) := (\mathcal{M}_p(D), \mathcal{F}(D, \mathcal{M}_p(D)))$  remains non-private.

*Proof.* We adopt RDP in this proof. Let  $\mathcal{M}_p : \mathcal{D} \rightarrow \mathcal{R}_1$  be a non-private (pre-trained) model (see (3)), and  $\mathcal{F} : \mathcal{D} \times \mathcal{R}_1 \rightarrow \mathcal{R}_2$  be any mechanism. We show that the composed mechanism  $\mathcal{M}_r : \mathcal{D} \rightarrow \mathcal{R}_1 \times \mathcal{R}_2, D \mapsto (\mathcal{M}_p(D), \mathcal{F}(D, \mathcal{M}_p(D)))$  remains non-private.

Indeed, fix any  $\epsilon > 0$  and choose  $D, D'$  such that

$$\mathbb{D}_\alpha(\mathcal{M}_p(D) \parallel \mathcal{M}_p(D')) > \epsilon, \quad (8)$$

which is possible due to  $\mathcal{M}_p$  being non-private.

Let  $P$  and  $Q$  denote the density of  $\mathcal{M}_p(D)$  and  $\mathcal{M}_p(D')$ , respectively. Applying the decomposition rule (see the proof of Proposition 1 in [31]), we obtain

$$\mathbb{D}_\alpha(\mathcal{M}_r(D) \parallel \mathcal{M}_r(D')) = \frac{1}{\alpha-1} \log \mathbb{E}_{Z \sim Q} \left[ \left( \frac{P(Z)}{Q(Z)} \right)^\alpha \underbrace{\exp \left( (\alpha-1) \mathbb{D}_\alpha(\mathcal{F}(D, Z) \parallel \mathcal{F}(D', Z)) \right)}_{\geq 1} \right] \quad (9)$$

$$\geq \frac{1}{\alpha-1} \log \mathbb{E}_{Z \sim Q} \left[ \left( \frac{P(Z)}{Q(Z)} \right)^\alpha \right] = \mathbb{D}_\alpha(\mathcal{M}_p(D) \parallel \mathcal{M}_p(D')) > \epsilon, \quad (10)$$

where the inequality follows from the fact that Rényi's  $\alpha$ -divergence is always nonnegative (when  $\alpha > 1$ ).

Since  $\epsilon$  is arbitrary, we have proved that  $\mathcal{M}_r$  remains non-private.  $\square$

**Theorem 3.1.** Each update step in the decoder  $S_\phi$  in stage 2 satisfies  $(\alpha, \frac{2\alpha}{\sigma^2})$ -RDP.

*Proof.* Let  $g_\phi$  be the gradient function of decoder  $S_\phi$ . Consider two adjacent batches  $d, d'$  of size  $B$  that only differs in the  $m$ -th entry  $(X_m, y_m), (X'_m, y'_m)$ , where  $1 \leq m \leq B$ . Let  $\bar{g}_\phi(d) = \frac{1}{B} \sum_{i=1}^B g_\phi(X_i, y_i)$ , then  $\tilde{g}_\phi$  on line 14 of stage 2 becomes:

$$\tilde{g}_\phi = \bar{g}_\phi(d) + \mathcal{N}(0, (\sigma C/B)^2 \mathbb{I}) \quad (11)$$

As  $\|g_\phi(X_i, y_i)\|_2 \leq C$  for all  $i$ , we know:

$$\Delta_2 \bar{g}_\phi = \max_{d, d'} \|\bar{g}_\phi(d) - \bar{g}_\phi(d')\|_2 \quad (12)$$

$$= \max_{(X_m, y_m), (X'_m, y'_m)} \frac{1}{B} \|g_\phi(X_m, y_m) - g_\phi(X'_m, y'_m)\|_2 \leq \frac{2C}{B}. \quad (13)$$

Then by Gaussian mechanism (Definition 2.3), we know each update step in the decoder (releasing  $\tilde{g}_\phi$ ) satisfies  $(\alpha, \frac{\alpha(\Delta_2 \bar{g}_\phi)^2}{2(\sigma C/B)^2})$ -RDP, i.e.  $(\alpha, \frac{2\alpha}{\sigma^2})$ -RDP.  $\square$

## B Datasets

We briefly introduce the public datasets and associated preprocessing. Image size is shown in  $\#channels \times height \times width$ . Images are normalized to the range of  $[0, 1]$ .

**MNIST [34] & Fashion MNIST [35]:** MNIST contains hand-written digits images, whereas Fashion MNIST contains cloth and shoe images. Images in both datasets are single-channel, in the size of  $1 \times 28 \times 28$ , and have 10 classes. We adopt the official training and test split.

**CelebA [36]:** CelebA is a dataset including face images of celebrities. Each image is in the size of  $3 \times 178 \times 218$  and has 40 binary attributes. All images are cropped to  $3 \times 178 \times 178$ , and then resized to  $3 \times 32 \times 32$ . We also adopt the official training and test split, but randomly select 60k images from training split as our training set.

## C Implementation

### C.1 Architecture & hyperparameters

Our conditional VAE code is adapted from a [public repo](#), where the architecture sequentially contains input layer, encoder, linear layers (for mean and variance, respectively), decoder input layer, decoder, and a final layer. The variation mainly lies in the number of hidden units and the number of convolutional layers in both encoder and decoder, as well as the number of latent dimensions. For MNIST and Fashion MNIST, we use two convolutional layers with 512 and 256 hidden units in both encoder and decoder, along with 8 latent dimensions. For CelebA, we use three convolutional layers with 512, 256 and 128 hidden units in both encode and decoder, along with 16 latent dimensions.

### C.2 Privacy implementation

We use a public repo, i.e. [pyvacy](#), for implementing DP training algorithm and epsilon calculation. Pyvacy tracks the privacy loss by RDP accountant, which is a PyTorch implementation based on [Tensorflow Privacy](#).

### C.3 Fréchet Inception Distance (FID)

FID calculates the distance between the feature vectors extracted by InceptionV3 pool3 layer [47] on real and synthetic samples. Specifically,

$$\text{FID} = \|\mu_r - \mu_g\|_2^2 + \text{Tr}(\Sigma_r + \Sigma_g - 2(\Sigma_r \Sigma_g)^{\frac{1}{2}}) \quad (14)$$

where  $X_r \sim \mathcal{N}(\mu_r, \Sigma_r)$  and  $X_g \sim \mathcal{N}(\mu_g, \Sigma_g)$  are activations of InceptionV3 pool3 layer of real images and generated images, respectively, and  $\text{Tr}(A)$  refers to the trace of a matrix  $A$ . Intuitively, a lower FID means the generation  $X_g$  is more realistic (or more similar to  $X_r$ ). We use a [PyTorch implementation](#) for computing FID, which will resize images and repeat channels three times for grayscale images to meet the input size requirement.

### C.4 Classification task

We follow Cao et al. [41] for the classifier implementation. We import scikit-learn package for implementation logistic regression classifier (e.g. from `sklearn.linear_model` import `LogisticRegression`) with default parameter settings.

The MLP network consists of following layers: `linear(input_dim, 100) → ReLU → linear(100, output_dim) → Softmax`.

The CNN consists of following layers: `Conv2d(input_channels, 32, kernel_size=3, stride = 2, padding=1) → Dropout(p=0.5) → ReLU → Conv2d(32, 64, kernel_size=3, stride = 2, padding=1) → Dropout(p=0.5) → ReLU → flatten → linear(flatten_dim, output_dim) → Softmax`.

Both MLP and CNN are optimized by Adam with default parameters. All classifiers are trained on synthetic data, and we report test accuracy on real test data as the evaluation metric.

### C.5 Baselines

All results of DP-MERF [39] are obtained by running their [code](#) with default parameters. It is worth mentioning that DP-MERF does not implement on CelebA. We adapt their code on CelebA by using the generative network they designed for SVHN with 16, 8, 8 channels for three convolutional layers, respectively.

GS-WGAN only implements on  $(10, 10^{-5})$ -DP. To target  $(1, 10^{-5})$ -DP, we tried two vanilla variations by tuning parameters of  $(10, 10^{-5})$ -DP in their [code](#), i.e. increasing noise scale while keeping the rest parameters unchanged, or decreasing the number of iterations while keeping the rest parameters unchanged. We experimentally found that both variations will not generate meaningful images. The former variation is not even able to generate anything on Fashion MNIST, so we instead present the latter variation for comparison.

All other results (e.g. numbers in the tables, generated images) are cited from papers as we specify. It is worth mentioning that DP-Sinkhorn, as a SoTA method under weak privacy constraints, has not released code yet, so we directly cite their results.

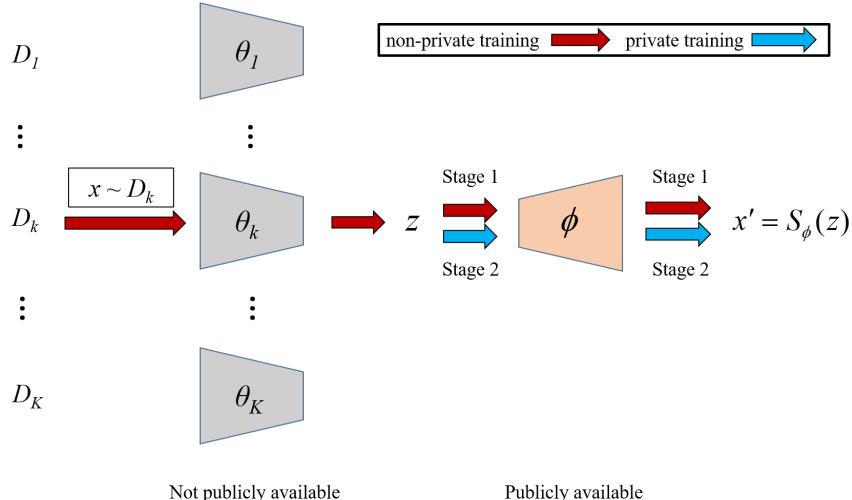


Figure 6: The two-stage strategy of training a DP<sup>2</sup>-VAE. In stage 1, we (non-privately) pre-train encoder  $T_{\theta_i}$  along with a new decoder  $S_\phi$  on private input  $D_i$  (for  $i = 1, 2, \dots, K$ ). In stage 2, we only load pre-trained encoders, and reinitialize the decoder in the beginning, then we train the  $S_\phi$  from scratch with private training algorithm while keeping updating encoders normally.

## D Framework

The schematic of DP<sup>2</sup>-VAE is depicted in Figure 6. In stage 1, we normally pre-train each encoder with a reinitialized decoder. In stage 2, we only transfer the pre-trained weights of encoders, and reinitialize the decoder in the beginning, then we train the decoder from scratch by private training algorithm while normally updating encoders.

## E Additional results

### E.1 Results on CelebA under $(10, 10^{-5})$ -DP

Figure 7 shows the qualitative comparison when  $\epsilon = 10$ . As opposed to DataLens and DP-MERF that generate blurry images, and DP-Sinkhorn that seems to generate "mean-like" face images, our method generates more informative and more diverse face images than baselines. Although DP-Sinkhorn targets  $(10, 10^{-6})$ -DP for celebA, while our method as well as DataLens and DP-MERF targets  $(10, 10^{-5})$ -DP, we remark that the difference in the noise multiplier in these two cases is small in our privacy implementation. Quantitatively, FID of our generation is 249.9, and CNN Acc is 80.7.

### E.2 Results under $(0.2, 10^{-5})$ -DP

We present additional qualitative and quantitative results under stronger privacy guarantee, i.e.  $\epsilon = 0.2$ , as shown in Figure 8. It is not surprising that generation becomes much worse in this case compared to  $\epsilon = 1$  or 10, because the noise multiplier is much larger under this stronger DP guarantee. Nevertheless, DP<sup>2</sup>-VAE can still generate meaningful instances and yield acceptable utility in downstream tasks across different datasets.

### E.3 Learning rate

As learning rate impacts the model convergence, we also include how FID and generated images vary with different learning rates. Figure 9 shows such comparison on MNIST under  $(10, 10^{-5})$ -DP (we remark that the variation trends on other datasets are similar to Figure 9). It is suggested that a too large or too small

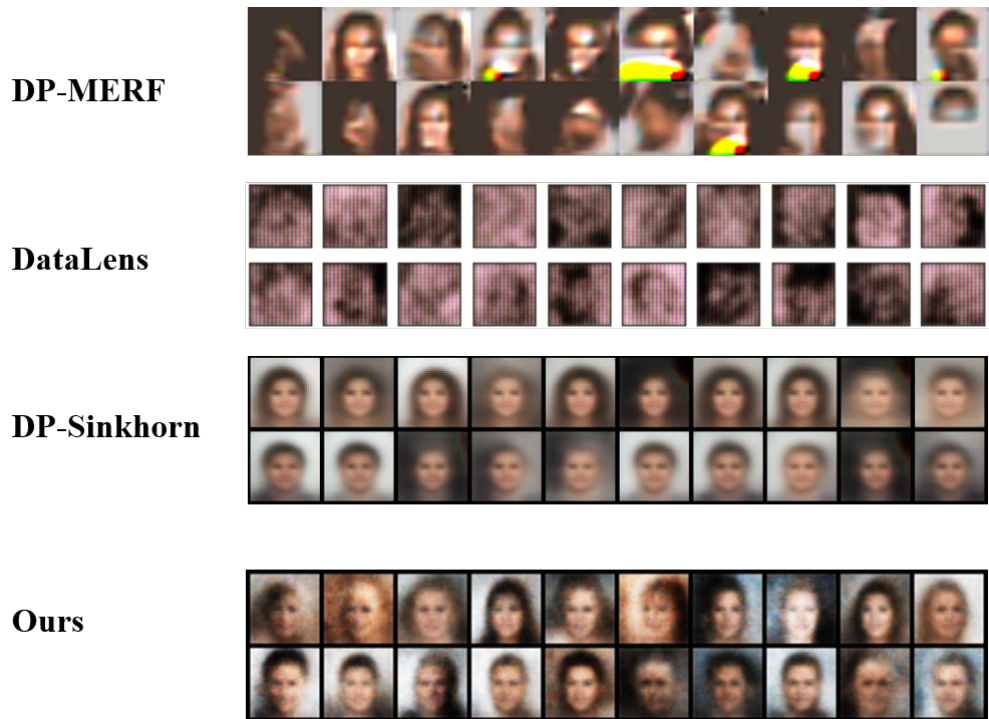


Figure 7: Qualitative comparison on CelebA conditioned on gender when  $\epsilon = 10$ . Images of DataLens and DP-Sinkhorn are cited from their papers, respectively. Top row: female. Bottom row: male.

learning rate is detrimental to training our model properly. We use learning rate as  $1 \times 10^{-4}$ , as it results in the best learning outcome on all three datasets.

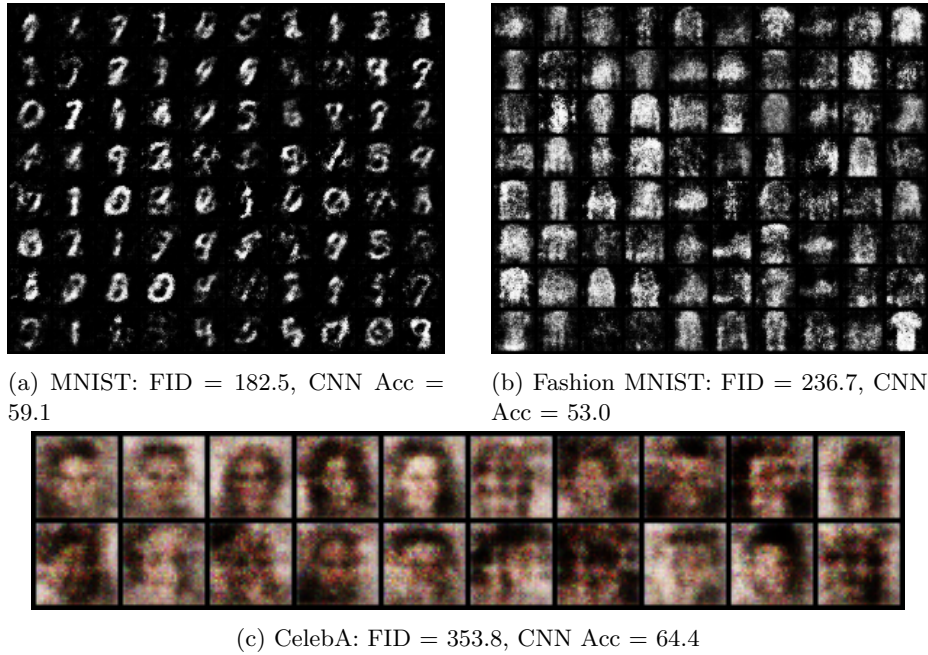


Figure 8: Results of DP<sup>2</sup>-VAE under  $(0.2, 10^{-5})$ -DP.

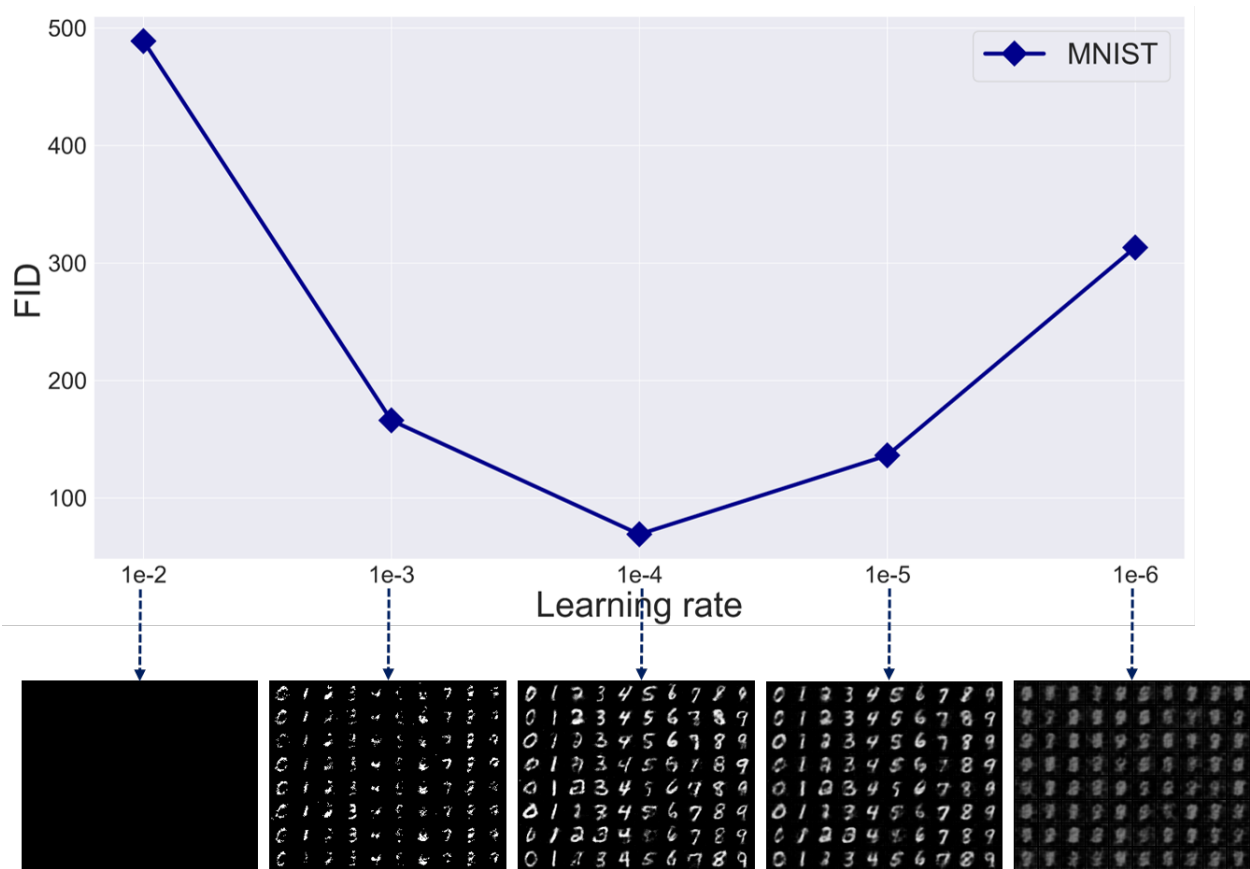


Figure 9: Generation quality v.s. learning rates under  $(10, 10^{-5})$ -DP